



Original

Noninvasive monitoring of muscle atrophy and bone metabolic disorders using dual-energy X-ray absorptiometry in diabetic mice

Kazuhiisa KISHI^{1)*}, Momo GOTO^{1)*}, Yoshiharu TSURU²⁾ and Masatoshi HORI¹⁾

¹⁾Department of Veterinary Pharmacology, Graduate School of Agriculture and Life Sciences, The University of Tokyo, 1-1-1 Yayoi, Bunkyo-ku, Tokyo 113-8657, Japan

²⁾Primetech Life Science Laboratory, Primetech Corporation, 1-3-25 Koishikawa, Bunkyo-ku, Tokyo 112-0002, Japan

Abstract: Tracking metabolic changes in skeletal muscle and bone using animal models of diabetes mellitus (DM) provides important insights for the management of DM complications. In this study, we aimed to establish a method for monitoring changes in body composition characteristics, such as fat mass, skeletal muscle mass (lean mass), bone mineral density, and bone mineral content, during DM progression using a dual-energy X-ray absorptiometry (DXA) system in a mouse model of streptozotocin (STZ)-induced type 1 DM. In the DM model, STZ administration resulted in increased blood glucose levels, increased water and food intake, and decreased body weight. Serum insulin levels were significantly decreased on day 30 of STZ administration. The DXA analysis revealed significant and persistent decreases in fat mass, lower limb skeletal muscle mass, and bone mineral content in DM mice. We measured tibialis anterior (TA) muscle weight and performed a quantitative analysis of tibial microstructure by micro-computed tomography imaging in DM mice. The TA muscle weight of DM mice was significantly lower than that of control mice. In addition, the trabecular bone volume fraction, trabecular thickness, trabecular number, and cortical thickness were significantly decreased in DM mice. Pearson's product-moment correlation coefficient analysis showed a high correlation between the DXA-measured and actual body composition. In conclusion, longitudinal measurement of body composition changes using a DXA system may be useful for monitoring abnormalities in muscle and bone metabolism in animal models of metabolic diseases such as DM mice.

Key words: animal welfare, diabetes mellitus, osteoporosis, sarcopenia

Introduction

Diabetes mellitus (DM) is one of the most prevalent metabolic diseases worldwide, and prevention of vascular complications such as diabetic retinopathy and diabetic nephropathy is a challenge. In addition, the progression of DM is associated with a variety of diseases other than vascular complications, such as musculoskeletal disorders and cancer [1–4]. In fact, DM induces decreases in skeletal muscle mass and bone density, triggering sarcopenia and osteoporosis [5–7]. However, our knowl-

edge of the pathophysiology of muscle and bone metabolism associated with the progression of DM is limited because of the difficulty of continuously monitoring multiple metabolic abnormalities in mice and other small animals. To conduct such studies, a noninvasive method is needed that can be used to evaluate changes in body composition with DM progression over time.

In recent years, dual-energy X-ray absorptiometry (DXA) has attracted much attention as a noninvasive method for assessing body composition characteristics, including muscle mass and bone density, in mice [8, 9].

(Received 19 July 2022 / Accepted 10 August 2022 / Published online in J-STAGE 15 September 2022)

Corresponding authors: K. Kishi. email: kishi0627@g.ecc.u-tokyo.ac.jp

M. Hori. email: horimasa@g.ecc.u-tokyo.ac.jp

*These authors contributed equally to this work.



This is an open-access article distributed under the terms of the Creative Commons Attribution Non-Commercial No Derivatives (by-nc-nd) License <<http://creativecommons.org/licenses/by-nc-nd/4.0/>>.

A recent study showed that DXA can be used to noninvasively detect changes in muscle mass due to disuse atrophy [10]. In addition, an obesity-related study showed that DXA can be used to assess relative changes in body fat mass and muscle mass due to abnormal mitochondrial function [11]. On the other hand, previous studies related to DM have been limited to evaluation in chronic animal models with advanced DM [12, 13]. Therefore, it is unclear whether DXA can accurately monitor the metabolic changes associated with DM progresses. To obtain a comprehensive understanding of the pathogenesis of DM and its complications, it is important to evaluate changes in muscle and bone metabolism over time in addition to blood glucose levels and insulin secretion capacity. Considering that DXA can rapidly and conveniently provide quantitative data on body composition in mice [14], it may be the most suitable method to evaluate muscle and bone changes over time as DM progresses.

Here, we applied DXA to DM model mice to test whether DXA is useful for detecting changes in body composition during the progression of DM. The results indicate that DXA can sensitively detect changes in body composition that occur in the early stages of DM in mice. DXA may be a useful *in vivo* method for simultaneous and quantitative monitoring of changes in muscle and bone metabolism in DM mice.

Materials and Methods

Animals

Male C57BL/6J mice (8–10 weeks) were used in this study. The mice were housed in sterile cages at 3 mice per 330 cm² and kept at 22 ± 2°C with a 12 h light/dark cycle. The mice were also allowed *ad libitum* access to water and standard mouse feed (MF, Oriental Yeast Co., Ltd., Tokyo, Japan). The experimental procedures using mice were conducted in accordance with the Guide for Animal Experiments of the University of Tokyo. All experimental procedures were approved by the Institutional Review Board of the University of Tokyo (approval code P18-131).

Diabetic mouse model

We used streptozotocin (STZ, FUJIFILM Wako Pure Chemical, Tokyo, Japan) to prepare a type 1 DM (T1DM) mouse model [15]. The STZ was dissolved in an ice-cold 0.1 M citrate buffer and intraperitoneally (ip) injected at 160 mg/kg. Control mice received the same amount of citrate buffer by ip injection. Blood glucose levels were measured using a LabAssay glucose kit (FUJIFILM Wako Pure Chemical); the onset of DM was determined

by hyperglycemia (>250 mg/dl). Blood samples were collected from the tail vein. Since DM mice were used in this study, their health status characteristics, including movement and fur condition, were monitored 3–4 times a week. In addition, the cages were cleaned frequently to maintain a clean environment, since DM mice exhibit polydipsia. In this study, we set a humane endpoint for the development of DM: if the rate of weight loss exceeded 20% within a few days after STZ administration, the mice were euthanized at that time. All animals were euthanized by cervical dislocation under deep isoflurane. No animals died before meeting the criteria for euthanasia.

Dual-energy X-ray absorptiometry

DXA was performed in accordance with previous reports [16, 17]. The body composition of each mouse was measured using a cone-beam flat-panel DXA detector (iNSiGHT VET DXA, Osteosys, Seoul, Korea). The mice were immobilized by gas inhalation (isoflurane). Fat mass, lean mass, and bone mass were quantified based on the attenuation of two different X-ray energy levels. Regions of interest (ROIs) were applied to the lower limbs of each mouse, and fat mass, lean mass, and bone mass were calculated for the lower regions of the right and left lower limbs. To confirm the accuracy of the data obtained by DXA, correlations with actual measurements obtained from autopsy experiments were evaluated by Pearson's product-moment correlation coefficient analysis.

Micro-computed tomography imaging

Micro-computed tomography (microCT) imaging was performed to measure morphometric and densitometric properties of murine bone, as described in previous reports [18, 19]. In this study, the analysis site in microCT was the tibia. Each sample was scanned using a microCT instrument (DELPet μ CT-100, DELBio, Taoyuan, Taiwan) under the following conditions: 40 kV, 375 μ A, 7.5 μ m voxel size, and 512 projections/180° rotation. Image reconstruction was performed using dedicated software (DELPet 3D Reconstruction Software, DELBio).

Standard morphometric analysis

Morphometric analysis of trabecular and cortical bone was performed using visualization and analysis software (Amira 4.6.0, FEI SAS, Thermo Fisher Scientific, Waltham, MA, USA). For trabecular and cortex measurements, a volume of interest (VOI) of 1.5 mm (200 pixels) was selected. The starting point of the VOI in the longitudinal direction was identified using the slice containing the lateral sides of the growth plate. Segmentation was

performed using a one-level threshold calculated for each image as the average of the gray levels corresponding to the bone and background peaks in the image histogram. The bone volume (BV) fraction was calculated by dividing the BV by the total volume (TV). For analysis of trabecular bone, the trabecular bone volume fraction (Tb.BV/TV), thickness (Tb.Th), separation (Tb.Sp), and number (Tb.N) were calculated. For analysis of cortical bone, the total cross-sectional area (Tt.Ar), cortical bone area (Ct.Ar), cortical area fraction (Ct.Ar/Tt.Ar), and average cortical thickness (Ct.Th) were calculated.

Blood chemistry tests

Blood samples for measuring insulin and insulin-like growth factor 1 (IGF-1) levels were obtained by cardiac puncture at the endpoint. Collected blood samples were incubated at room temperature for 2 h and then centrifuged at $2,000 \times g$ for 15 min at 4°C . The supernatant obtained by this centrifugation was used as the serum sample. The serum was evaluated for the hormones IGF-1 and insulin. The serum levels of these hormones were determined using a Mouse/Rat IGF-1 Quantikine ELISA Kit (MG100, R&D Systems, Minneapolis, MN, USA) and a Mouse Insulin ELISA Kit (10-1247-01, Merck, Winston-Salem, NC, USA). The experimental procedures were conducted in accordance with the instructions of the assay kit.

Statistical analysis

The numerical data were expressed as the mean \pm SD. Statistical differences were analyzed by unpaired Student's *t* test for comparisons between two groups. Statistical significance was defined as $P < 0.05$. Pearson's product-moment correlation coefficient analysis was used to evaluate the correlations between data. The following variable (*t*) was derived using correlation coefficient (*r*) follows Student's *t*-distribution with $n-2$ degrees of freedom, so the two-tailed *P* value could be obtained from it.

$$t = r \sqrt{\frac{n-2}{1-r^2}}$$

All statistical analyses were performed using GraphPad Prism (version 9.3.1, GraphPad Software, San Diego, CA, USA).

Results

STZ induces hyperglycemia and metabolic abnormalities, including water and food intake abnormalities

We first monitored the conditions of mice after STZ

administration over time to evaluate the metabolic changes caused by the onset of DM. STZ administration markedly increased the blood glucose levels of mice after 1 week (Fig. 1A). The body weights of STZ-treated mice gradually decreased with increasing blood glucose levels (Fig. 1B). An increase in blood glucose and a decrease in body weight are typical metabolic changes suggesting the development of T1DM.

In addition, water intake and food intake were measured over time as indicators of the effect of DM on nutritional status. Water intake and food intake in control mice were similar during all observation periods. On the other hand, in STZ-treated mice, water and food intake increased significantly with the onset of DM (Figs. 1C and D). These results suggest that the onset of T1DM is characterized by abnormal drinking and feeding accompanied by hyperglycemia and weight loss, which can affect body composition.

DXA simultaneously detects abnormalities in skeletal muscle and bone metabolism in diabetic mice

Next, we applied the DXA system to DM mice to determine if changes in body composition could be detected continuously. Mice were maintained in the prone position under isoflurane anesthesia (Fig. 2A). DXA simultaneously provided quantitative data on fat mass, skeletal muscle mass (lean mass), bone mineral density, and bone mineral content in mice (Figs. 2B–E). In control mice, all body composition parameters remained constant or increased with growth (Figs. 2D and E). In contrast, fat mass and skeletal muscle mass decreased in DM mice 2 days after STZ administration (Fig. 2D). These decreases were likely attributable to a temporary decrease in food intake due to STZ administration, and this interpretation was supported by the data on food intake in DM mice. Subsequently, fat mass and skeletal muscle mass in the lower limbs of DM mice persistently decreased with the progression of DM (Fig. 2D).

In addition to fat mass and skeletal muscle mass, DXA quantitatively detected changes in bone mineral density and bone mineral content in murine tibias (Fig. 2E). The values of these bone parameters were significantly lower in DM mice than in control mice (Fig. 2E). These results suggest that DXA helps enable simultaneous and continuous monitoring of abnormalities in skeletal muscle and bone metabolism in DM mice.

Progression of T1DM induces skeletal muscle atrophy and osteopenia with reduced insulin signaling

Insulin signaling is a powerful cell proliferation signal, and a decrease in this signal induces muscle atrophy

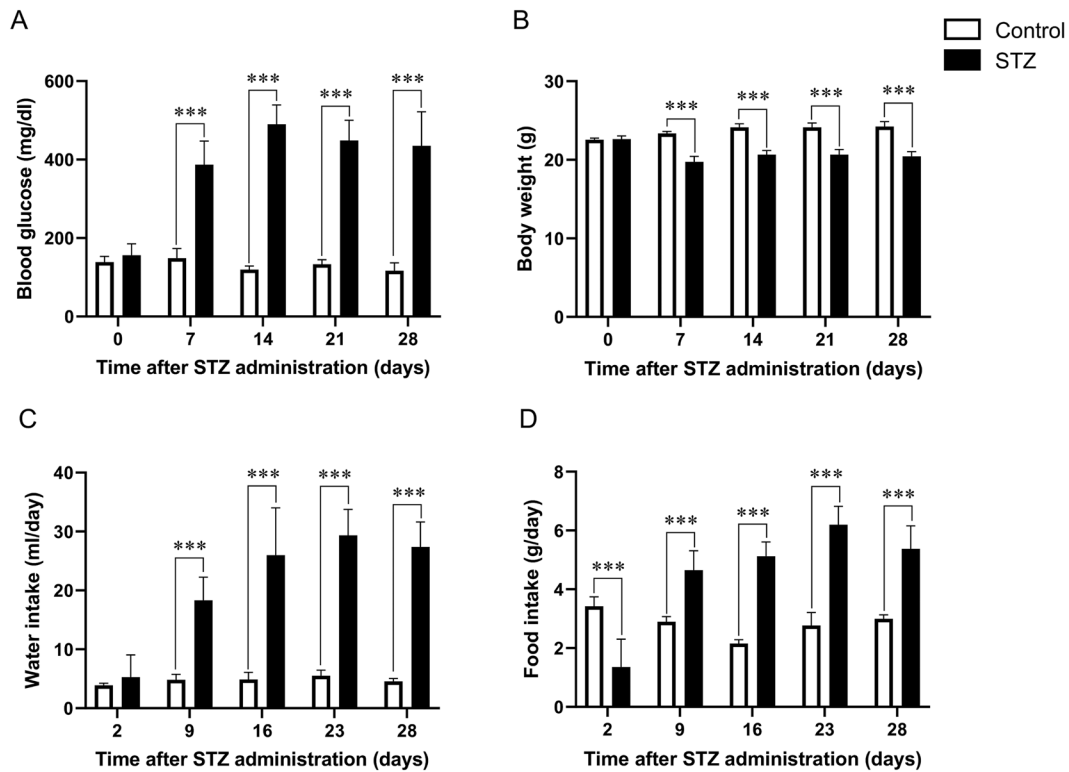


Fig. 1. Progression of type 1 diabetes mellitus (T1DM) and metabolic abnormalities after streptozotocin (STZ) administration in mice. (A, B) Blood glucose levels and body weight after STZ administration in mice. Hyperglycemia and weight loss are typical metabolic changes suggestive of the development of T1DM. Each column shows the mean \pm SD ($n=5-7$). (C, D) Changes in water intake and food intake in diabetic mice. Each column shows the mean \pm SD ($n=5-7$). *** $P<0.005$; significantly different from control.

and osteopenia [20–22]. Therefore, we considered that the decreases in skeletal muscle and bone parameters in T1DM mice detected by DXA may have been due to altered insulin signaling. We focused on the hormones that regulate insulin signaling, insulin and IGF-1, and measured serum concentrations of these hormones in DM mice 4 weeks after STZ administration. Serum insulin levels were significantly decreased in DM mice (Fig. 3A). Serum IGF-1 concentrations in DM mice were not significantly different from the concentrations in control mice (Fig. 3B). These results suggested that the decreases in serum insulin levels may lead to decreases in the values of skeletal muscle and bone parameters.

Then, to determine whether skeletal muscle and bone metabolism were actually abnormal in DM mice, the weight of the tibialis anterior (TA) muscle was quantified. The weight of TA muscle excised by necropsy was significantly reduced in DM mice (Fig. 3C). Bone microstructure was assessed by microCT (Fig. 3D), and normal bone microstructure characteristics, including trabecular and cortical bone characteristics, were observed in control mice. On the other hand, DM mice had thinner cortical bone and a reduced trabecular bone area, a finding suggestive of reduced bone mass (Fig. 3E). In

fact, the Tb.BV/TV, Tb.Th, Tb.N, and Ct.Th were significantly decreased in DM mice, suggesting reduced bone mass (Fig. 3F). Furthermore, Tb.Sp was significantly increased in DM mice compared with control mice as trabecular bone decreased (Fig. 3F). These results suggest that the progression of T1DM leads to muscle atrophy and osteopenia with decreased insulin signaling.

DXA measurements are strongly correlated with actual measurements in diabetic mice

Metabolic abnormalities in body composition occur in T1DM mice, and DXA may accurately reflect these changes. Finally, we performed a Pearson's product-moment correlation coefficient analysis on fat mass and skeletal muscle mass to clarify the correlation between DXA-provided body composition data and actual measurements in DM mice. The total body fat mass estimated by DXA correlated with the weight of epididymal fat (Fig. 4A). Skeletal muscle mass was determined by the weight of the right and left tibialis anterior (TA) muscles. The lean mass quantified as the skeletal muscle mass in the DXA data correlated with the TA muscle weight (Fig. 4B). Additionally, we examined the correlation between the values of bone parameters measured by

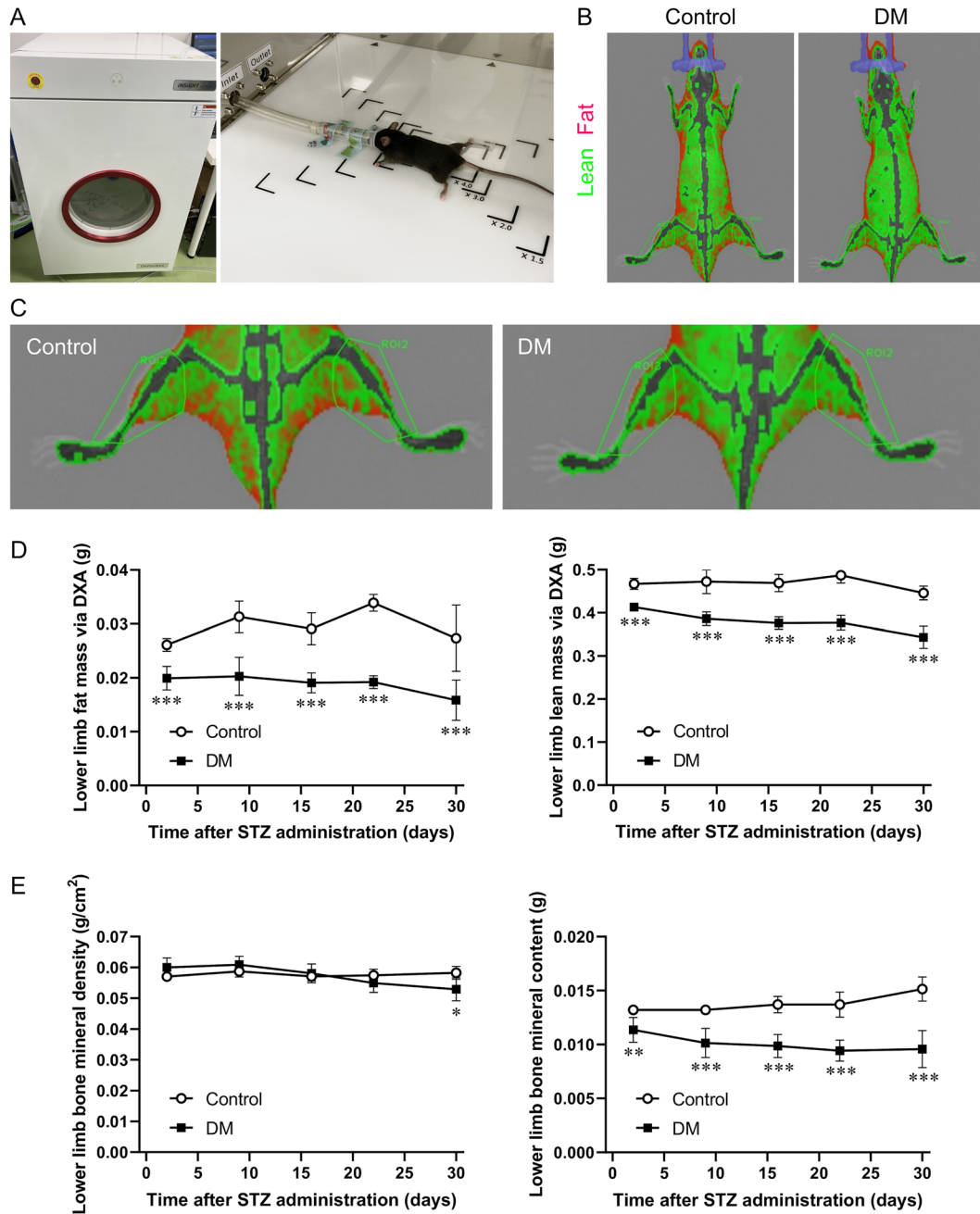


Fig. 2. Analysis of changes in body composition in diabetes mellitus (DM) mice via dual-energy X-ray absorptiometry (DXA). (A) DXA system used in this study. All mice were placed in the abdominal position with their legs extended under isoflurane anesthesia. (B, C) DXA scan images of control and DM mice. DXA can visualize fat (red) and lean mass (green) in mice. The green box shows the region of interest (ROI) for the lower limb body composition analysis. (D) Fat mass and lean mass of the lower limbs in control and DM mice obtained via DXA. Each column shows the mean \pm SD ($n=5-7$). (E) Bone mineral density and bone mineral content of lower limbs in control and DM mice obtained via DXA. These body composition measurements were conducted on days 2, 9, 16, 22, and 30 after streptozotocin (STZ) administration. Each symbol shows the mean \pm SD ($n=5-7$). * $P<0.05$, ** $P<0.01$, *** $P<0.005$; significantly different from control.

DXA and those measured by CT. Bone mineral content in the DXA data correlated with the BV estimated by CT (Fig. 4C). These results suggest that DXA-provided body composition data accurately reflect changes in body composition in DM mice.

Discussion

In this study, we tested the usefulness of DXA as an *in vivo* method for tracking changes in muscle and bone metabolism in DM mice. Administration of STZ induced T1DM in mice, causing metabolic disorders, such as

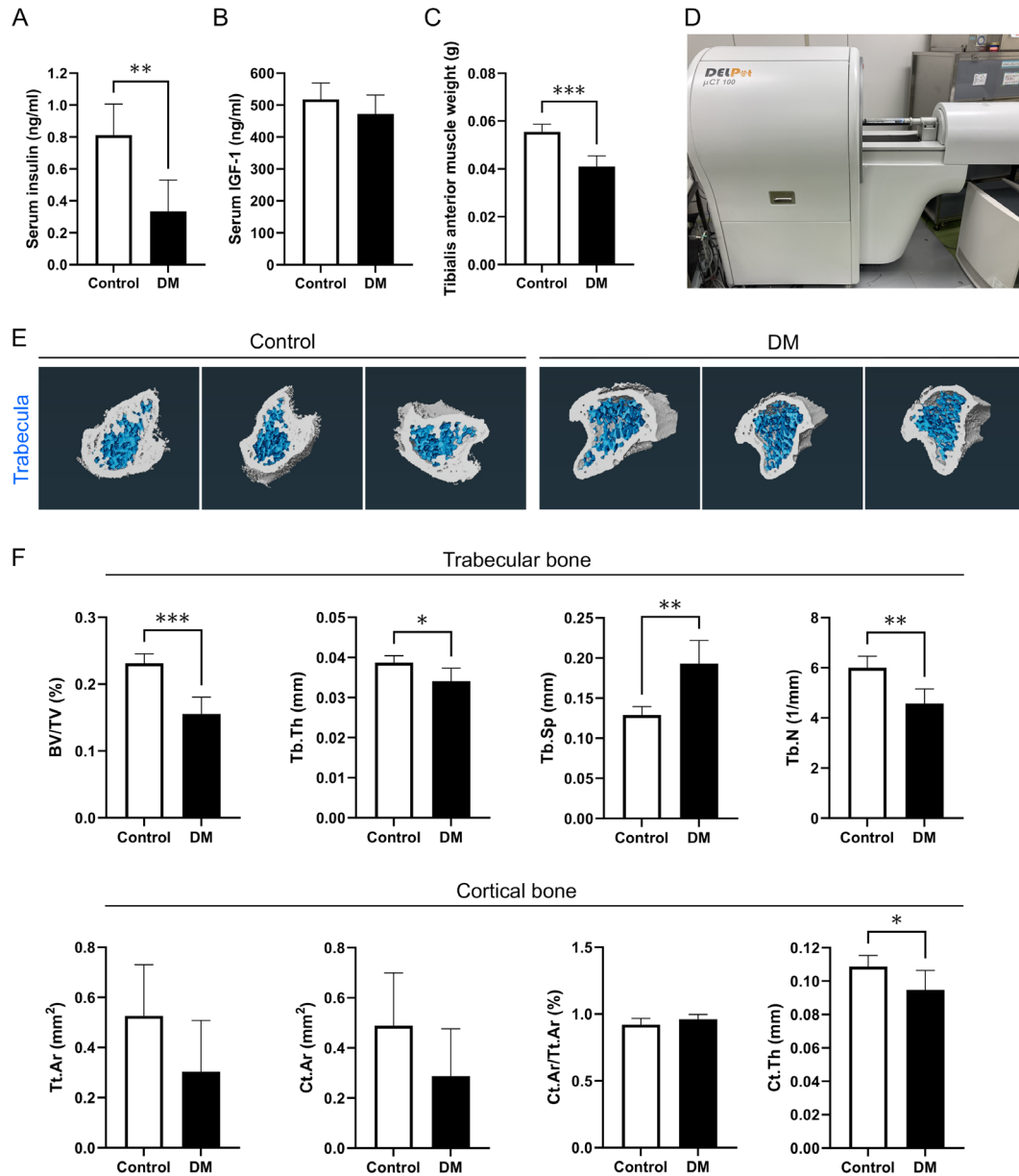


Fig. 3. Muscle atrophy and osteopenia due to progression of diabetes mellitus (DM) in mice. (A, B) Serum insulin and insulin-like growth factor (IGF-1) levels in control and DM mice on day 30 after streptozotocin (STZ) administration. Each column shows the mean \pm SD ($n=5-7$). (C) Weight of tibialis anterior (TA) muscle in control and DM mice on day 30 after STZ administration. Each column shows the mean \pm SD ($n=4-6$). (D) MicroCT imaging system used in this study. The tibiae of mice 30 days after STZ administration were measured by this system. (E) Representative images of the microstructure of the tibia in control and DM mice determined via micro-computed tomography (microCT). The blue area in the image shows the trabecula. (F) Microstructural analysis of trabecular and cortical bone in murine tibiae using microCT. For analysis of trabecular bone, the trabecular bone volume fraction (Tb.BV/TV), thickness (Tb.Th), separation (Tb.Sp), and number (Tb.N) were calculated. For analysis of cortical bone, the total cross-sectional area (Tt.Ar), cortical bone area (Ct.Ar), cortical area fraction (Ct.Ar/Tt.Ar), and average cortical thickness (Ct.Th) were calculated. In (C) and (F), the data for each sample were calculated by averaging the values for both feet. Each column shows the mean \pm SD ($n=5-6$). * $P<0.05$, ** $P<0.01$, *** $P<0.005$; significantly different from control.

hyperglycemia, insulin deficiency, hyperphagia, and increased water intake. DXA enabled noninvasive and quantitative detection of changes in body composition caused by these metabolic disorders. Importantly, DXA was able to simultaneously detect decreased muscle mass

and bone density in mice at risk for sarcopenia and osteoporosis. Furthermore, we demonstrated that body composition data obtained via DXA correlated with epididymal fat and TA muscle weight in mice. These findings suggest that the data provided by DXA can be

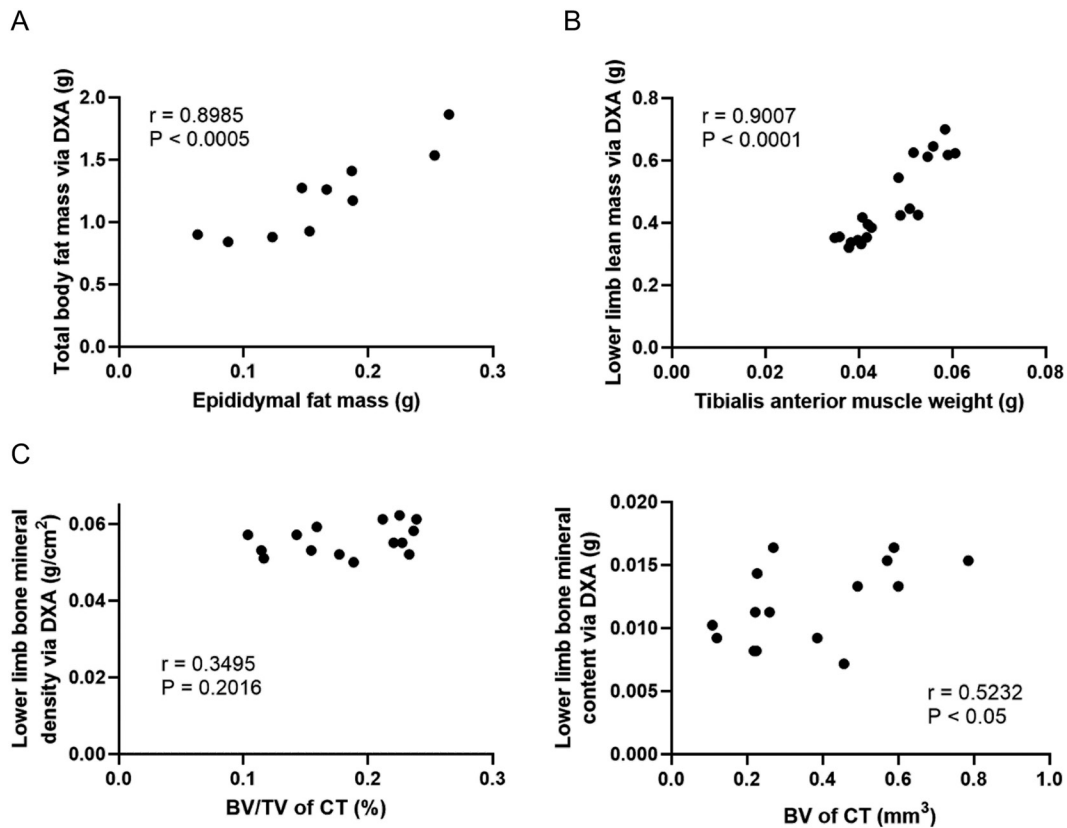


Fig. 4. Correlation between measured data and dual-energy X-ray absorptiometry (DXA)-estimated data for murine body composition. (A) Correlation between the actual measured weight of epididymal fat and the total body fat mass measured by DXA in mice. (B) Correlation between the actual measured weight of tibialis anterior (TA) muscles and the lower limb lean mass measured by DXA in mice. (C) Correlation between the lower limb bone data measured by CT and that measured by DXA in mice. Pearson's product-moment correlation coefficient analysis was used to evaluate the correlations between the data. Two-tailed P values were calculated by GraphPad Prism.

used to determine metabolic changes with the progression of DM in mice. This study provides new insights into how to monitor muscle and bone metabolic disorders in metabolic disease model animals such as DM mice.

DM induces muscle atrophy and osteopenia [5–7]. In recent years, its significant risks and the need for therapeutic intervention have been recognized. Basic research on mice helps elucidate physiological parameters for therapeutic intervention [23]. We found that DXA sensitively detects changes in muscle mass and bone parameters in the early stages of DM in mice. Several reports have shown that mice with reduced insulin signaling have reduced muscle mass and bone density [20–22]. Hyperglycemia is associated with the development of frailty and limited athletic performance, which are due to loss of muscle mass [24]. Consistent with these findings, this study showed that serum insulin levels in DM mice were significantly reduced and that muscle mass and bone parameters were concomitantly reduced. The decreases in muscle mass and bone parameters in DM mice are likely due to hyperglycemia and insulin defi-

ciency. In addition, we found that the data obtained from excised organs and microCT supported the conclusion that DXA is sufficiently accurate to detect these changes. In clinical practice, DXA is a commonly used body composition assessment method, and its data correlate with data obtained from the gold standards: computed tomography (CT) and magnetic resonance imaging (MRI) [25–29]. These findings suggest that the data obtained from DXA accurately reflect changes in body composition in DM mice.

To evaluate changes in body composition in metabolic diseases such as DM, continuous monitoring of body composition is required [30]. In preclinical studies, microCT designed primarily for small animals has been used for high-definition bone structure analysis and muscle mass assessment [31, 32]. However, continuous use of CT and MRI is limited because the steps, including examination, image processing, and analysis, take considerable time. To address this issue, we proposed continuous monitoring using DXA. Data production via DXA is much faster than that via CT or MRI. In addition,

DXA has a lower radiation dose than CT, and its exposure dose is negligible [33]. These advantages could contribute not only to tracking of the body compositions of DM mice over time but also to assessment of the durations of action and therapeutic effects of drugs. DXA accurately detects DM-related changes in body composition in preclinical studies, which may be useful for assessment of preventive and therapeutic interventions for DM complications.

The methods used in both basic research and clinical trials facilitate the extrapolation of data from preclinical studies to the clinic. The data obtained from DXA could be highly reproducible in humans and would be more attractive than those obtained by invasive methods. In addition, noninvasive methods such as DXA are expected to contribute to improving the quality of animal experiments. Interest in animal welfare is growing worldwide, and reducing the number and burden of animals used in experiments is an important task [34]. One useful feature of DXA is its ability to evaluate changes in body composition quickly and over time in the same individual. This reduces the number of animals used in studies and improves the quality of life of the animals. Application of DXA in animal experiments will contribute to both clinical extrapolation and the basic principles of animal experiments.

The muscle data used for DXA in this study were limited to weight only, and weight estimates can vary with glycogen and water content [35]. DM increases daily water and food intake, which may affect DXA estimates. Although this study shows that DXA estimates correlate with actual TA muscle weights in DM mice, this effect should be taken into account when interpreting DXA-derived muscle mass in DM model animals. Furthermore, even though both CT and DXA sensitively detected reduced bone parameters in DM mice, the correlation between the values of bone mineral density measured by CT and those measured by DXA was not high. The reason for this may be the different dimensions for comparison: DXA measures only bone weight and area, whereas CT measures BV. In addition, DXA is a radiation-based diagnostic imaging method similar to CT and may not be suitable for longitudinal studies with radiation-sensitive juveniles. On the other hand, in clinical practice, DXA is frequently used to evaluate body composition in newborns and children [36, 37]. Much remains unclear about the effects of long-term use of DXA on the body compositions of small animals. Further research is needed to determine the continuous conditions of use for DXA. In recent years, DXA has been used to monitor the body compositions of model mice to learn more about lifestyle-related diseases [11,

16, 38]. In the future, if the usefulness and safety of DXA are proven in various disease model animals, it may be possible to conclusively show that DXA is a useful method for monitoring metabolic changes in mice.

In conclusion, we demonstrated that DXA is a useful technique that can accurately monitor changes in body composition in DM mice. Monitoring body composition in DM mice is a crucial approach to understanding the functional links between DM and locomotor disorders. Simultaneous detection of changes in muscle and bone metabolism via DXA is expected to enable in vivo monitoring of preventive and therapeutic strategies for locomotor disorders in DM. DXA will be a useful metabolic measurement method for translational research that can be safely and easily performed in animals.

Acknowledgments

This work was supported by a Grant-in-Aid for Scientific Research from the Ministry of Education, Culture, Sports, Science and Technology (24248050 to MH) and a Grant-in-Aid for JSPS Fellows (20J11240 to KK). The authors have declared that no competing interests exist.

References

- Izzo A, Massimino E, Riccardi G, Della Pepa G. A Narrative Review on Sarcopenia in Type 2 Diabetes Mellitus: Prevalence and Associated Factors. *Nutrients*. 2021; 13: E183. [\[Medline\]](#) [\[CrossRef\]](#)
- Wong E, Backholer K, Gearon E, Harding J, Freak-Poli R, Stevenson C, et al. Diabetes and risk of physical disability in adults: a systematic review and meta-analysis. *Lancet Diabetes Endocrinol*. 2013; 1: 106–114. [\[Medline\]](#) [\[CrossRef\]](#)
- Giovannucci E, Harlan DM, Archer MC, Bergenstal RM, Gapstur SM, Habel LA, et al. Diabetes and cancer: a consensus report. *Diabetes Care*. 2010; 33: 1674–1685. [\[Medline\]](#) [\[CrossRef\]](#)
- Lega IC, Lipscombe LL. Review: Diabetes, Obesity, and Cancer-Pathophysiology and Clinical Implications. *Endocr Rev*. 2020; 41: bnz014. [\[Medline\]](#) [\[CrossRef\]](#)
- Kalyani RR, Corriere M, Ferrucci L. Age-related and disease-related muscle loss: the effect of diabetes, obesity, and other diseases. *Lancet Diabetes Endocrinol*. 2014; 2: 819–829. [\[Medline\]](#) [\[CrossRef\]](#)
- Napoli N, Chandran M, Pierroz DD, Abrahamsen B, Schwartz AV, Ferrari SL. IOF Bone and Diabetes Working Group. Mechanisms of diabetes mellitus-induced bone fragility. *Nat Rev Endocrinol*. 2017; 13: 208–219. [\[Medline\]](#) [\[CrossRef\]](#)
- Shanbhogue VV, Hansen S, Frost M, Brixen K, Hermann AP. Bone disease in diabetes: another manifestation of microvascular disease? *Lancet Diabetes Endocrinol*. 2017; 5: 827–838. [\[Medline\]](#) [\[CrossRef\]](#)
- Bazzocchi A, Ponti F, Albinini U, Battista G, Guglielmi G. DXA: Technical aspects and application. *Eur J Radiol*. 2016; 85: 1481–1492. [\[Medline\]](#) [\[CrossRef\]](#)
- Gargiulo S, Gramanzini M, Megna R, Greco A, Albanese S, Manfredi C, et al. Evaluation of growth patterns and body composition in C57Bl/6J mice using dual energy X-ray absorptiometry. *BioMed Res Int*. 2014; 2014: 253067. [\[Medline\]](#) [\[CrossRef\]](#)

10. Lee SJ, Lehar A, Meir JU, Koch C, Morgan A, Warren LE, et al. Targeting myostatin/activin A protects against skeletal muscle and bone loss during spaceflight. *Proc Natl Acad Sci USA*. 2020; 117: 23942–23951. [[Medline](#)] [[CrossRef](#)]
11. Kang GM, Min SH, Lee CH, Kim JY, Lim HS, Choi MJ, et al. Mitohormesis in Hypothalamic POMC Neurons Mediates Regular Exercise-Induced High-Turnover Metabolism. *Cell Metab*. 2021; 33: 334–349.e6. [[Medline](#)] [[CrossRef](#)]
12. Rivoira M, Rodríguez V, Picotto G, Battaglini R, Tolosa de Talamoni N. Naringin prevents bone loss in a rat model of type 1 Diabetes mellitus. *Arch Biochem Biophys*. 2018; 637: 56–63. [[Medline](#)] [[CrossRef](#)]
13. Ortinau LC, Linden MA, Dirkes R, Rector RS, Hinton PS. Obesity and type 2 diabetes, not a diet high in fat, sucrose, and cholesterol, negatively impacts bone outcomes in the hyperphagic Otsuka Long Evans Tokushima Fatty rat. *Bone*. 2017; 105: 200–211. [[Medline](#)] [[CrossRef](#)]
14. Brommage R. Validation and calibration of DEXA body composition in mice. *Am J Physiol Endocrinol Metab*. 2003; 285: E454–E459. [[Medline](#)] [[CrossRef](#)]
15. Lenzen S. The mechanisms of alloxan- and streptozotocin-induced diabetes. *Diabetologia*. 2008; 51: 216–226. [[Medline](#)] [[CrossRef](#)]
16. Cole CL, Beck CA, Robinson D, Ye J, Mills B, Gerber SA, et al. Dual Energy X-ray Absorptiometry (DEXA) as a longitudinal outcome measure of cancer-related muscle wasting in mice. *PLoS One*. 2020; 15: e0230695. [[Medline](#)] [[CrossRef](#)]
17. Yeu J, Ko HJ, Kim D, Ahn Y, Kim J, Lee W, et al. Evaluation of iNSiGHT VET DXA (Dual-Energy X-ray Absorptiometry) for assessing body composition in obese rats fed with high fat diet: a follow-up study of diet induced obesity model for 8 weeks. *Lab Anim Res*. 2019; 35: 2. [[Medline](#)] [[CrossRef](#)]
18. Bouxsein ML, Boyd SK, Christiansen BA, Guldberg RE, Jepsen KJ, Müller R. Guidelines for assessment of bone microstructure in rodents using micro-computed tomography. *J Bone Miner Res*. 2010; 25: 1468–1486. [[Medline](#)] [[CrossRef](#)]
19. Oliviero S, Lu Y, Viceconti M, Dall'Ara E. Effect of integration time on the morphometric, densitometric and mechanical properties of the mouse tibia. *J Biomech*. 2017; 65: 203–211. [[Medline](#)] [[CrossRef](#)]
20. Luo J, Sobkiw CL, Hirshman MF, Logsdon MN, Li TQ, Goodyear LJ, et al. Loss of class IA PI3K signaling in muscle leads to impaired muscle growth, insulin response, and hyperlipidemia. *Cell Metab*. 2006; 3: 355–366. [[Medline](#)] [[CrossRef](#)]
21. Fulzele K, Riddle RC, DiGirolamo DJ, Cao X, Wan C, Chen D, et al. Insulin receptor signaling in osteoblasts regulates postnatal bone acquisition and body composition. *Cell*. 2010; 142: 309–319. [[Medline](#)] [[CrossRef](#)]
22. Ferron M, Wei J, Yoshizawa T, Del Fattore A, DePinho RA, Teti A, et al. Insulin signaling in osteoblasts integrates bone remodeling and energy metabolism. *Cell*. 2010; 142: 296–308. [[Medline](#)] [[CrossRef](#)]
23. Rosenthal N, Brown S. The mouse ascending: perspectives for human-disease models. *Nat Cell Biol*. 2007; 9: 993–999. [[Medline](#)] [[CrossRef](#)]
24. Kalyani RR, Tian J, Xue QL, Walston J, Cappola AR, Fried LP, et al. Hyperglycemia and incidence of frailty and lower extremity mobility limitations in older women. *J Am Geriatr Soc*. 2012; 60: 1701–1707. [[Medline](#)] [[CrossRef](#)]
25. Bredella MA, Ghomi RH, Thomas BJ, Torriani M, Brick DJ, Gerweck AV, et al. Comparison of DXA and CT in the assessment of body composition in premenopausal women with obesity and anorexia nervosa. *Obesity (Silver Spring)*. 2010; 18: 2227–2233. [[Medline](#)] [[CrossRef](#)]
26. Marlatt KL, Greenway FL, Ravussin E. Assessment of EchoMRI-AH versus dual-energy X-ray absorptiometry by iDXA to measure human body composition. *Eur J Clin Nutr*. 2017; 71: 558–560. [[Medline](#)] [[CrossRef](#)]
27. Levine JA, Abboud L, Barry M, Reed JE, Sheedy PF, Jensen MD. Measuring leg muscle and fat mass in humans: comparison of CT and dual-energy X-ray absorptiometry. *J Appl Physiol* 1985. 2000; 88: 452–456. [[Medline](#)]
28. Müller MJ, Braun W, Pourhassan M, Geisler C, Bosy-Westphal A. Application of standards and models in body composition analysis. *Proc Nutr Soc*. 2016; 75: 181–187. [[Medline](#)] [[CrossRef](#)]
29. Silver HJ, Niswender KD, Kullberg J, Berglund J, Johansson L, Bruvold M, et al. Comparison of gross body fat-water magnetic resonance imaging at 3 Tesla to dual-energy X-ray absorptiometry in obese women. *Obesity (Silver Spring)*. 2013; 21: 765–774. [[Medline](#)] [[CrossRef](#)]
30. Prado CM, Heymsfield SB. Lean tissue imaging: a new era for nutritional assessment and intervention. *JPEN J Parenter Enteral Nutr*. 2014; 38: 940–953. [[Medline](#)] [[CrossRef](#)]
31. Chiou AE, Liu C, Moreno-Jiménez I, Tang T, Wagermaier W, Dean MN, et al. Breast cancer-secreted factors perturb murine bone growth in regions prone to metastasis. *Sci Adv*. 2021; 7: eabf2283. [[Medline](#)] [[CrossRef](#)]
32. Pasetto L, Olivari D, Nardo G, Trolese MC, Bendotti C, Piccirillo R, et al. Micro-computed tomography for non-invasive evaluation of muscle atrophy in mouse models of disease. *PLoS One*. 2018; 13: e0198089. [[Medline](#)] [[CrossRef](#)]
33. Toombs RJ, Ducher G, Shepherd JA, De Souza MJ. The impact of recent technological advances on the trueness and precision of DXA to assess body composition. *Obesity (Silver Spring)*. 2012; 20: 30–39. [[Medline](#)] [[CrossRef](#)]
34. Carbone L. Estimating mouse and rat use in American laboratories by extrapolation from Animal Welfare Act-regulated species. *Sci Rep*. 2021; 11: 493. [[Medline](#)] [[CrossRef](#)]
35. Bone JL, Ross ML, Tomcik KA, Jeacocke NA, Hopkins WG, Burke LM. Manipulation of Muscle Creatine and Glycogen Changes Dual X-ray Absorptiometry Estimates of Body Composition. *Med Sci Sports Exerc*. 2017; 49: 1029–1035. [[Medline](#)] [[CrossRef](#)]
36. Mughal MZ, Eelloo J, Roberts SA, Maresh M, Ward KA, Ashby R, et al. Body composition and bone status of children born to mothers with type 1 diabetes mellitus. *Arch Dis Child*. 2010; 95: 281–285. [[Medline](#)]
37. Shepherd JA, Sommer MJ, Fan B, Powers C, Stranix-Chibanda L, Zadzilka A, et al. Advanced Analysis Techniques Improve Infant Bone and Body Composition Measures by Dual-Energy X-Ray Absorptiometry. *J Pediatr*. 2017; 181: 248–253.e3. [[Medline](#)] [[CrossRef](#)]
38. Jensen CH, Kosmina R, Rydén M, Baun C, Hvidsten S, Andersen MS, et al. The imprinted gene Delta like non-canonical notch ligand 1 (*Dlk1*) associates with obesity and triggers insulin resistance through inhibition of skeletal muscle glucose uptake. *EBioMedicine*. 2019; 46: 368–380. [[Medline](#)] [[CrossRef](#)]